Modulated Magnetic Structures of $ErPb_3$, $HoPb_3$, $ErTl_3$ and $HoTl_3$

K. Knorr*, A. Loidl*, and B. Stühn*
Institut für Physik der Universität, Mainz, Federal Republic of Germany

J.L. Buévoz**
Institut Laue-Langevin, Grenoble, France

Neutron diffraction experiments have been carried out on the magnetically ordered phases of $ErPb_3$, $HoPb_3$, $ErTl_3$ and $HoTl_3$. The magnetic moments were found to be sinusoidally modulated with a propagation vector of (0, 0.2, 0.5) for the Pb-compounds and (0.38, 0.38, 0.16) for the Tl-compounds.

1. Introduction

One of the most fascinating phenomena in the field of magnetism is the appearance of oscillatory spin structures like spirals or longitudinal static spin waves (LSW). In the hexagonal lattice of the heavy rare earth (RE) metals these structures occur quite naturally as a consequence of *(i)* the axial anisotropy of the crystal electric field (CF), which forces the spins either into the *c*-direction or into the basal plane and *(ii)* of the long range oscillatory exchange interactions which couples the moments of a basal plane, which are all parallel, to neighbouring planes [1]. In cubic RE-compounds complex arrangements of spins occur less frequently. Recently the existence of a modulated LSW-structure was established for the compound $CeAl_2$ [2], with some controversy whether the modulation should be described by a single [2] or a triple-**q** structure [3].

The rare earth compounds of the present study crystallize in the simple Cu_3Au-structure ($L1_2$-type). The magnetic RE-ions form a primitive cubic lattice. By alloying to various non-magnetic metals (In, Pb, Tl, Sn, Pt), with different numbers of valence electrons, one can hope to influence the electric band schemes which in turn determine the magnetic properties via the CF and the exchange interaction.

The original intent of the present study was to investigate the directions and magnitudes of the ordered moments to verify the CF-parameters determined by Groß et al. [4]. In analogy to the isomorphic heavy $REIn_3$ compounds we expected simple antiferromagnetic structures with propagation vectors $\mathbf{q}_0=(0,\ 1/2,\ 1/2)$ [5, 6]. Instead we observed LSW-structures in all four compounds whose moments partially disagree with the predictions of a mean field calculation based on the CF-parameters of [4].

2. Experimental Results

The phase diagrams of the systems are unknown, but by extrapolating from the phase diagrams of other RE-Pb systems [7], in particular of the neighbour system Dy-Pb we have deduced that the melting temperatures of the compounds of the present study are at about 1,000 °C and the peritectic formation of the Cu_3Au phases takes place at about 800 °C. The samples were prepared by sealing amounts of the elements corresponding to a stoichiometry of $REX_{3.1}$ in Ta crucibles and heating them to 1,200 °C well above the inferred melting temperatures. The small excess of non-transition metal *X* (Pb resp. Tl) is intended to suppress the possible formation of parasitic RE-rich phases like e.g., REX_2. The purity of the starting materials was 4N for Er and Ho and 5N for Pb and Tl. After the fusion the compounds were annealed for two days at 750 °C, a temperature which was somewhat below the expected peritectic temperatures. Since the sam-

* Work supported by the Bundesministerium für Forschung und Technologie

** Present adress: CNET BP 42, 38240 MEYLAN France

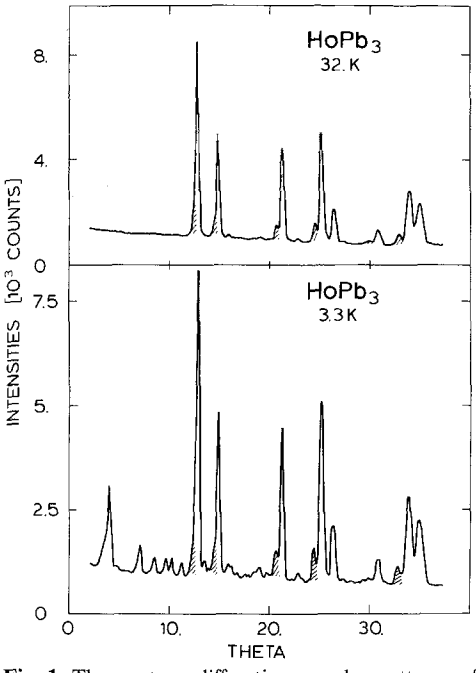

Fig. 1. The neutron diffraction powder patterns of $HoPb_3$ in the paramagnetic and the magnetically ordered phase. The shaded areas indicate the contributions of percipitated elementary Pb

ples deteriorate rapidly when exposed to air, they were stored in evacuated glass ampoules and crushed into powder in an argon atmosphere shortly before the start of the neutron diffraction experiments. Obviously the protection against oxidation failed in the case of $ErTl_3$, since strong lines due to the presence of sesquioxide Er_2O_3 were identified in the powder pattern as will be discussed later.

Approximately 10 grms of the powdered specimens were filled into vanadium tubes and mounted into a variable temperature cryostat. The diffraction experiments were carried out on the diffractometer D2 of the Institut Laue-Langevin. The wavelength of the incident neutrons was 1.22 Å. Two powder spectra covering Bragg angles Θ from 2° to 40° were recorded for each sample well above and below the magnetic ordering temperature T_N (given in Table 3). In Fig. 1 the spectra of $HoPb_3$ are shown as an example. The Figs. 2–5 cover the low Θ part of the difference patterns $I(T<T_N)-I(T>T_N)$ for each of the four compounds. The raw spectra (Fig. 1) were dominated by the strong nuclear reflections of the Cu_3Au-structure, whose structure factor F_{hkl} is proportional to $b_{RE}+3b_X$ (h, k, l all even or all odd). Their intensities did not change when crossing T_N. Consequently there is no ferromagnetic component and they cancel in the difference patterns. The other type of nuclear reflections with a geometrical structure factor proportional to the difference of the scattering lengths $b_{RE}-b_X$ were too weak to be observed in the experiment ($b_{Pb}=0.9404$, $b_{Tl}=0.890$; $b_{Er}=0.800$, $b_{Ho}=0.85$). In all raw spectra additional reflections of the elementary metals fcc Pb resp, hcp Tl were present: they are indicated by the shaded areas of Fig. 1. Their appearance is due to the excess of these materials used in the preparation. Of course, these parasitic powder lines disappear in the difference intensities, too. The strong asymmetric shape of the powder lines at small Bragg angles is due to the finite height of the detector (umbrella effect).

3. Analysis of the Experimental Results

In a first step the angular positions of the magnetic reflections were indexed, assuming that the magnetic structure can be described by a single propagation vector $\mathbf{q}_0$. The magnetic Bragg reflections τ_m occur at the satellite positions of the reciprocal lattice points τ_{hkl} of the cubic structure, with $\tau_m \equiv (hkl)^{\pm} = \tau_{hkl} \pm \mathbf{q}_0$. The search for the correct propagation vector was done with a computer by carying $\mathbf{q}_0$ through the irreducible part of the Brillouin zone of the simple cubic lattice. In particular we did not impose

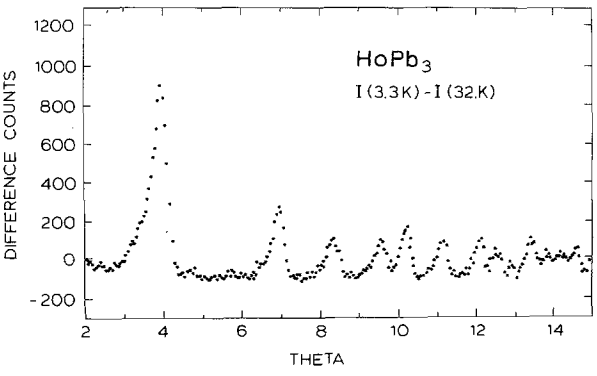

Fig. 2. The difference pattern of $HoPb_3$ at low Bragg angles

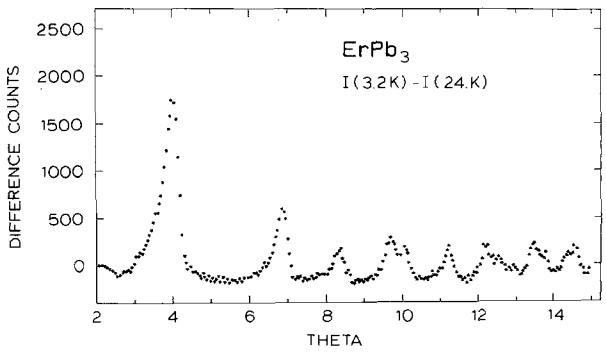

Fig. 3. The difference pattern of $ErPb_3$

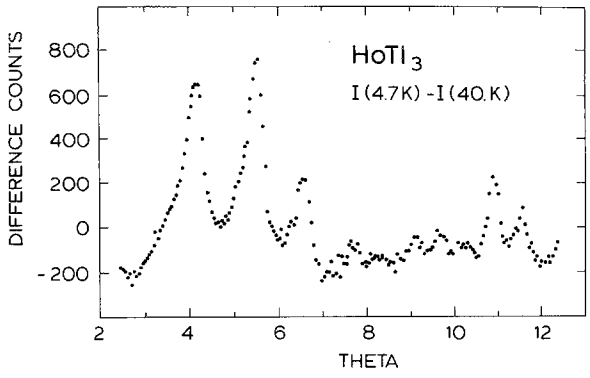

Fig. 4. The difference pattern of $HoTl_3$

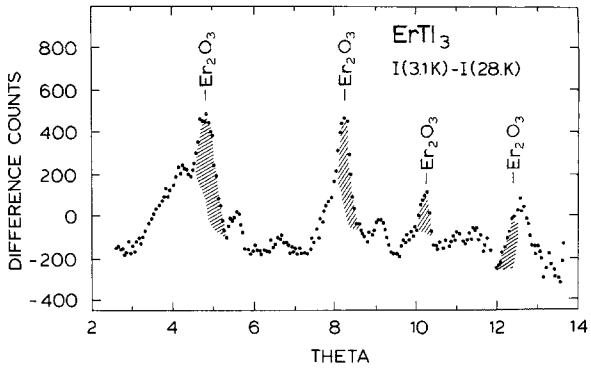

Fig. 5. The difference pattern of $ErTl_3$. The shaded areas are interpreted as contributions of Er_2O_3

the restriction (although, finally this turned out to be the case) that the first reflection is the $(000)^{\pm}$ Debye-Scherrer ring. For $ErPb_3$, $HoPb_3$ and $HoTl_3$ this procedure gave a clear result. All the lines of the diffraction patterns could be indexed by a unique vector $\mathbf{q}_0$ and all the lines predicted were found in the pattern. In the two Pb-compounds we found $\mathbf{q}_0 = (0, 0.2, 0.5)$ and for $HoTl_3$ $\mathbf{q}_0 = (0.38, 0.38, 0.16)$ in reduced reciprocal lattice units.

The uncertainty in the larger components of $\mathbf{q}_0$ is in the order of 0.01 and 0.03 in the smaller ones. The indexing of the spectrum of $ErTl_3$ caused some problems: Only after discarding the strongest lines in the difference pattern (shaded areas in Fig. 5) it was possible to find an unique propagation vector $\mathbf{q}_0$ which is then identical to that of $HoTl_3$. The extra reflections we identified as the (001), (112), (013) and (123) reflections of Er_2O_3 [8].

Obviously this sample had oxidized considerably, presumably during the procedure of crushing. We surmise that the two Pb-compounds as well as the two Tl-compounds have a common $\mathbf{q}_0$ independent of the RE-ion. Traces of higher Fourier components like $\tau_{hkl} \pm 3\mathbf{q}_0$ which are expected to occur in modulated structures at temperatures low compared to T_N due to a "squaring up" of the structure [1], have not been observed.

In the second part of the evaluation the intensities of the low temperature peaks were used to set up a model of the magnetic structure. The integrated intensities of the magnetic reflections were extracted from the difference patterns. These intensities were converted into values of the quantity F^2_{obs} which is the structure factor $F^2_{(hkl)^{\pm}}$ times multiplicity by considering the Lorentz factor, absorption corrections and magnetic form factors.

The variety of possible magnetic structures is very effectively reduced firstly by the experimental observation that there are no ferromagnetic contributions which would have shown up as additional scattered intensities on top of the nuclear reflections, and secondly by the fact that the RE-ions form a primitive cubic lattice. We therefore restricted ourselves to two models: The simple spiral and a collinear arrangement with sinusoidally modulated moments

$$\boldsymbol{\mu} = \boldsymbol{\mu}_0 \cos(\mathbf{q}_0 \cdot \mathbf{r})$$

The structure factor is then given by the relation [9]

$$F^2_{(hkl)^{\pm}} \sim \tfrac{1}{4}\mu_0^2(1 \pm \cos^2\varphi).$$

The positive sign is valid for the spiral, the negative sign for the LSW structure. μ_0 is the full magnitude of the magnetic moment, it is brought to absolute values by scaling to the intensities of the nuclear reflections. φ is the angle between $\tau_m \equiv (hkl)^{\pm}$ and the unique axis of the model, which is the common direction of the moments in the modulated structure resp. the axis of the spiral. Thus, both models have three free parameters, the length of the magnetic moments and the direction of the unique axis characterized by two angles. These free parameters were determined by least square fits. For $ErPb_3$, $HoPb_3$ and $HoTl_3$ the R-factors based on the configuration with modulated moments were about 3 times smaller than the R-factors based on the spiral structure. We therefore propose that the three compounds oder magnetically with sinusoidally modulated moments. The corresponding calculated and observed values for the peak positions as well as the calculated and observed magnetic form factors are listed in Tables 1 and 2. For $ErTl_3$ the agreement between experiment and theoretical model is considerably worse, yielding R-factors of the fits of the order of 30%. A clear destinction between the two models and a reliable determination of the parameters involved was impossible. Probably this negative result has to be explained by an inaccurate determination of the observed intensities of those magnetic satellite reflec-

Table 1. The assignment, the observed and calculated values of the peak positions and the observed and calculated intensities of the low angle magnetic Bragg reflections for $HoPb_3$ and $ErPb_3$

$(hkl)^{\pm}$	$HoPb_3$ (3.3 K)				$ErPb_3$ (3.2 K)			
	Θ_{calc}	Θ_{obs}	F^2_{calc}	F^2_{obs}	Θ_{calc}	Θ_{obs}	F^2_{calc}	F^2_{obs}
$(000)^+$ $(001)^-$	3.95	3.90	1.01	1.06 ± 0.02	3.95	4.00	1.00	1.10 ± 0.02
$(010)^-$ $(011)^-$	6.92	6.92	0.90	0.95 ± 0.04	6.94	6.87	1.00	0.86 ± 0.03
$(100)^{\pm}$ $(101)^-$ $(10\bar{1})^-$	8.35	8.35	0.79	0.70 ± 0.06	8.36	8.35	0.45	0.44 ± 0.04
$(010)^+$ $(01\bar{1})^+$	9.56	9.57	0.88	0.96 ± 0.07	9.58	9.65	1.00	1.13 ± 0.06
$(111)^-$ $(110)^-$ $(1\bar{1}0)^+$ $(1\bar{1}\bar{1})^+$	10.12	10.16	1.05	1.10 ± 0.09	10.14	10.05	0.94	0.90 ± 0.05
$(001)^+$ $(002)^-$	11.15	11.16	1.05	1.17 ± 0.10	11.17	11.23	1.00	0.96 ± 0.08
$(110)^+$ $(11\bar{1})^+$ $(1\bar{1}1)^-$ $(1\bar{1}0)^-$	12.10	12.11	1.24	1.26 ± 0.11	12.13	12.15	1.26	2.16 ± 0.10
$(01\bar{1})^-$ $(012)^-$	12.55	12.55	1.00	0.90 ± 0.12	12.58	12.50	1.00	
$(102)^-$ $(101)^+$ $(10\bar{1})^-$ $(10\bar{2})^+$	13.40	13.40	1.57		13.43	13.45	1.39	2.23 ± 0.12
$(020)^-$ $(021)^-$	13.81	13.85	0.86	4.78 ± 0.28	13.83	13.80	1.00	
$(011)^+$ $(01\bar{2})^+$	14.21	14.20	0.96		14.24	14.30	1.00	2.66 ± 0.16
$(1\bar{1}\bar{2})^+$ $(1\bar{1}1)^+$ $(112)^-$ $(11\bar{1})^-$	14.60	14.60	1.59		14.63	14.60	1.49	
$R=\frac{1}{N}\sum\frac{\lvert F^2_{obs}-F^2_{calc}\rvert}{F^2_{obs}}$			0.07				0.07	

Table 2. The assignment, the observed and calculated values of the peak positions and the observed and calculated intensities of the low angle magnetic Bragg reflections for $HoTl_3$ and $ErTl_3$ (for $ErTl_3$ only the peak positions are listed)

$(hkl)^{\pm}$	$HoTl_3$ (4.7 K)				$ErTl_3$ (3.1 K)	
	Θ_{calc}	Θ_{obs}	F^2_{calc}	F^2_{obs}	Θ_{calc}	Θ_{obs}
$(000)^+$	4.23	4.14	0.479	0.416 ± 0.016	4.24	4.20
$(100)^-$ $(010)^-$	5.62	5.55	0.773	0.848 ± 0.034	5.63	5.55
$(110)^-$	6.73	6.60	0.478	0.508 ± 0.030	6.75	6.65
$(001)^-$	7.53	7.67	0.199	0.220 ± 0.026	7.55	7.65
$(011)^-$ $(101)^-$	8.40	8.35	0.474	0.278 ± 0.065	8.42	
$(111)^-$	9.19	9.10	0.332	0.342 ± 0.038	9.21	9.10
$(001)^+$	9.68	9.67	0.191	0.416 ± 0.050	9.70	9.80
$(10\bar{1})^-$ $(01\bar{1})^-$	10.37	10.25	0.362	0.374 ± 0.048	10.40	
$(010)^+$ $(100)^+$	10.92	10.90	0.947	1.139 ± 0.057	10.94	11.00
$(11\bar{1})^-$	11.03		0.229		11.05	
$(110)^+$	11.54	11.55	0.816	0.859 ± 0.069	11.56	11.45
$R=\frac{1}{N}\sum\frac{\lvert F^2_{obs}-F^2_{calc}\rvert}{F^2_{obs}}$			0.18			

tions which are screened by the peaks of Er_2O_3 in Fig. 5. Because of these uncertainties we desist from presenting values for the calculated and observed intensities for $ErTl_3$. In Table 2 we list only the values for the peak positions.

A summary of the parameters (lattice constant a, Néel temperature T_N, ordering wave vector $\mathbf{q}_0$, magnetic structure, magnitude of the RE-moments $|\mu_0|$, and the direction of the RE-moments $\mu_0/|\mu_0|$) are listed in Table 3. The given directions of the RE-moments are the absolute minima of our fits, but these minima are rather broad distributions and the two angles determining the directions can be changed by approximately 5°–10° without striking changes in the R-factors.

For the Pb-compounds we followed in some detail the temperature dependence of the intensities of the magnetic satellite reflections, in order to detect changes in the propagation vector $\mathbf{q}_0$ or in the directions of the moments $\mu_0/|\mu_0|$. For both compounds $\mathbf{q}_0$ and $\mu_0/|\mu_0|$ remained constant from T_N down to the lowest temperatures reached in these experiments (3.2 K for $ErPb_3$ and 3.3 K for $HoPb_3$). The temperature dependence of the magnitude of the modulated moments, as derived from the experiment, are given in Fig. 6.

Table 3. The lattice constants a, the Néel temperatures T_N, the propagation vectors $\mathbf{q}_0$, the magnetic structure, the magnitude of the RE-moments $|\mu_0|$ and the direction of the moments $\mu_0/|\mu_0|$

	a (Å)	T_N (K)	$\mathbf{q}_0$	Magn. structure	$\lvert\mu_0\rvert$ (μ_B)	$\mu_0/\lvert\mu_0\rvert$
$ErPb_3$	4.763	4.5	(0, 0.2, 0.5)	LSW	8, 3 at 3.2 K	[100]
$HoPb_3$	4.773	7.0	(0, 0.2, 0.5)	LSW	8, 3 at 3.3 K	[0.9, 0.44, 0]
$ErTl_3$	4.628	6	(0.38, 0.38, 0.16)			
$HoTl_3$	4.673	7.5	(0.38, 0.38, 0.16)	LSW	8, 5 at 4.7 K	[0.29, −0.33, 0.9]

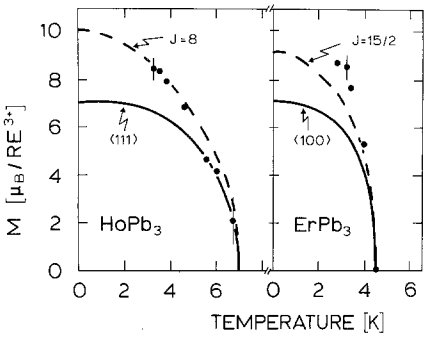

Fig. 6. The temperature dependence of the amplitude of the magnetic moment of the modulated structures for $HoPb_3$ and $ErPb_3$. The dashed lines give the Brillouin type magnetization for the free ion case, the solid lines are the result of a mean field calculation based on the CF level schemes of [4]

4. Discussion

The RE-ions in a metallic matrix experience various interactions *a)* the isotropic Heisenberg exchange which is mediated by the conduction electrons, *b)* a single ion anisotropy due to the CF and *c)* residual interactions like electric quadrupolar effects, the classical coupling of two magnetic dipoles and higher two ion anisotropy terms of the exchange interactions.

The exchange determines the translational symmetry of the spin structures by imposing a harmonic variation in the spin order which is characterized by the propagation vector $\mathbf{q}_0$. At sufficiently high temperatures close to T_N, $\mathbf{q}_0$ is the wave vector where the Fourier transform $J_{ex}(\mathbf{q})$ of the exchange coupling attains its absolute maximum. In the present cases the magnetic phases of the two Pb-compounds can be considered as commensurate with the nuclear lattice in the sense that the components of $\mathbf{q}_0$ are simple fractions or vice versa that an enlarged magnetic cell (a, 5a, 2a) can be constructed. The magnetic phases of the Tl-compounds on the contrary are incommensurate. The multiplicity of the star of $\mathbf{q}_0$ is 12 for the Pb- and 24 for the Tl-compounds. Phase transitions which involve oder parameters with such high dimensions are of great theoretical interest [10] and offer the chance of multiple-$\mathbf{q}_0$ structures.

The present propagation vectors require a delicate balance of the Fourier components in $J_{ex}(\mathbf{q})$. Decomposing $J_{ex}(\mathbf{q})$ into contributions from the N_i members of the shell of i^{th} neighbours with the coefficients J_i

$$J_{ex}(\mathbf{q}) = \sum_i \sum_{j=1}^{N_i} J_i \cos(\mathbf{q}\mathbf{r}_j)$$

one finds that an exchange coupling to the first and second neighbours only, which is quite an usual assumption and which already explains the complex spin structures of the heavy RE-metals, can generate maxima of $J_{ex}(\mathbf{q})$ at the following wave vectors (000), (1/2 0 0), (0 1/2 1/2), and (1/2 1/2 1/2). These propagation vectors represent the ferromagnetic and simple antiferromagnetic structures. The phase diagram is shown in Fig. 7 as a function of the ratio J_1/J_2. The propagation vectors of the present components can be obtained by including the coupling to further neighbours. The perhaps most straightforward way is to consider an interaction with the fourth neighbours at a distance 2a. The following relations between J_1, J_2 and J_4 are then deduced from the condition that the absolute maximum of $J_{ex}(\mathbf{q})$ occurs at the propagation vectors which were observed in the experiment: This yields for the

Pb-compounds

$J_1 > 0$, $J_2 < 0$ with $|J_2| \gg |J_1|$ and $J_4 = -0.81\,J_1$

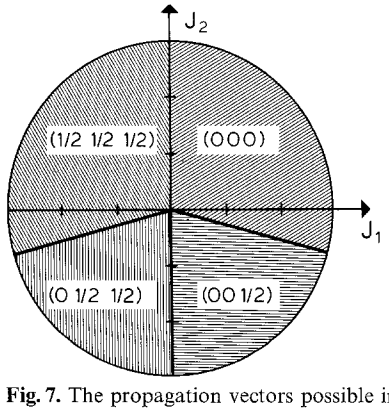

Fig. 7. The propagation vectors possible in a sc lattice of magnetic ions with an exchange coupling between first (J_1) and second (J_2) neighbours. The lower left phase is observed in the isomorphic $REIn_3$, the lower right phase in the $RESn_3$ compounds

and for the

Tl-compounds $J_1 < 0$, $J_2 = 0.542\, J_1$
and $J_4 = 0.271 J_1$.

A coupling to the first, second and third neighbours only, could not explain the modulations observed. Looking just at the relations between J_1 and J_2 one might regard the structure of the Tl-compounds as an offspring of the (0 1/2 1/2) type antiferromagnetism of the heavy $REIn_3$ systems whereas the structures of the two Pb-compounds are closely related to the (0 0 1/2) type antiferromagnetism which was observed in $PrSn_3$ and $NdSn_3$ [6]. These relations and the identity of the propagation vectors in $HoPb_3$ and $ErPb_3$ on one hand and in $HoTl_3$ and $ErTl_3$ on the other hand, mean that the electronic band structures of these systems are mainly determined by the non-magnetic constituents and depend little on the RE. In fact Tl and In are expected to contribute for three, Pb and Sn for four valence electrons. In this light it would be interesting to investigate the magnetic structures of the pseudobinary compounds like $RE(In, Pb)_3$.

It is clear that a sinusoidal arrangement has a high entropy. Thus, at some temperature which is usually of the order of $T_N/2$ [1] the structure should lower the free energy by squaring up approaching a regular antiphase domain pattern (unless the systems prefers to undergo a transition to a different magnetic structure of high symmetry like a ferromagnet). We were unable to detect higher harmonics of the propagation vector. Presumably this negative result is due to the relatively high temperatures where the experiments were carried out and to the large background of the powder patterns. In fact we estimated the higher harmonics to be at least one order of magnitude weaker than the pricipal satellites.

One expects that the direction and the amplitude of the magnetic moments should be mainly determined by the crystal field. Quite generally cubic fields favour structures where the spins are aligned along sets of equivalent main symmetry directions, ⟨100⟩, ⟨110⟩ or ⟨111⟩, rather than spirals which require a very small anisotropy within a plane. The CF's of several RE-intermetallic compounds with Cu_3Au structure are known from previous inelastic neutron scattering experiments [4]. Combining these results with the present ones we obtain very complete information on $HoPb_3$ and $ErPb_3$. We have carried out a mean field calculation of the spontaneous magnetization, the result is included in Fig. 6. For $ErPb_3$ the easy axis of the calculation agrees with the direction of the modulated moment, but the magnitude of the moment at 3.5 K is predicted to be $5\,\mu_B$ in contradiction to the value of $8.5\,\mu_B$ derived from the diffraction experiment. For $HoPb_3$ neither the direction nor the magnitude of the calculated magnetic moment agree with the results of the structure analysis. Following the mean field model $HoPb_3$ is on the verge of changing the easy axis from ⟨111⟩ to ⟨110⟩. The moments of the LSW structure point however into a low symmetry direction intermediate between [100] and [110]. Practically the same direction was observed in the antiferromagnetic structure of $HoIn_3$.

The apparent failure of the crystal field concept is surprising since the CF's of the compounds are strong compared to the exchange coupling as can be seen from the ratio of the CF-splitting and the ordering temperature. Thus there is a strong need for considering additional interactions. In this context we want to point out that the CF-ground states, Γ_8 resp. Γ_5, carry strong electric quadrupole moments which favour the occurence of magnetoelastic effects. In the three compounds where the spin structure could be derived from the diffraction results, the magnetic moments are within the experimental error always perpendicular to the propagation vector. This fact indicates that transverse two-ion-anisotropies play an important role in these compounds, though it is still hard to imagine how these effects can override the CF-single-ion-anisotropy.

References

1. Elliott, R.J.: Phys. Rev. **124**, 346 (1961)
2. Barbara, B., Boucherle, J.X., Buevoz, J.L., Rossignol, M.F., Schweizer, J.: Solid State Commun. **24**, 481 (1977)
   Barbara, B., Rossignol, M.F., Boucherle, J.A., Vettier, C.: Phys. Rev. Lett. **45**, 938 (1980)
3. Gurewitz, E., Shapiro, S.M., Kupterberg, L.C., Parks, R.D.: J. Appl. Phys. **50**, 2014 (1979)
   Shapiro, S.M., Gurewitz, E., Parks, R.D., Kupferberg, L.C.: Phys. Rev. Lett. **43**, 1748 (1979)
4. Groß, W., Knorr, K., Murani, A.P., Buschow, K.H.J.: Z. Phys. B - Condensed Matter **37**, 123 (1980)
5. Nereson, N., Arnold, G.: J. Chem. Phys. **53**, 2818 (1970)
6. Lethuillier, P., Pierre, J., Fillion, G., Barbara, B.: Phys. Status Solidi A **15**, 613 (1973)
7. Gschneidner, K.A., Jr., McMasters, O.D.: Monatsh. Chem. **101**, 1499 (1971)
8. Moon, R.M., Koehler, W.C., Child, H.R., Raubenheimer, L.J.: Phys. Rev. **176**, 722 (1968)
9. Koehler, W.C.: In: Magnetic Properties in Rare Earth Metals. Elliott, R.J. (ed.), pp. 81–128. NewYork: Plenum Press 1972
10. Bak, P.: J. Appl. Phys. **50**, 1970 (1979)

K. Knorr
A. Loidl
B. Stühn
Institut für Physik
Universität Mainz
Jakob-Welder-Weg 11
D-6500 Mainz
Federal Republic of Germany

J.L. Buévoz
Institut Max von Laue – Paul Langevin
156 X
F-38042 Grenoble Cedex
France